ZOOLOGICAL SCIENCE 6: 649–658 (1989)

Oscillations of Membrane Potential and Membrane Resistance during the Cell Cycle in the Newt Egg Macromeres

Eiji Sato and Shin-Ichi Tagawa

Department of Environmental Science, Division of Graduate School of Science and Technology, and Department of Biology, Faculty of Science, Kumamoto University, Kumamoto 860, Japan

ABSTRACT—The electrical characteristics of macromeres in newt eggs at the morula stage were examined electrically during the cell cycle, and the negative membrane potential (Em) and membrane resistance (Rm) were found to oscillate. For designation of the cell stage in the cell cycle, the time between cleavage-furrow formations was divided into 100 stages. The cell stage at which furrow formation occurred was designated St.50. The increase in Rm began from St.0 and reached a peak value at St.30. On the other had, the membrane showed hyperpolarization from St.10 to St.40 and then showed depolarization. After furrow formation, Rm continued to decrease and reached a minimum value at St.60, after which the value increased and showed a small peak at St.80. The membrane continued to depolarize from St.40 and reached a plateau level at around St.60. To investigate the mechanism of these electrical changes, an Na^+-K^+ pump inhibitor and high-Ca^{2+} solution were perfused to the macromeres. Despite the inhibition of the Na^+-K^+ pump, the membrane was hyperpolarized during the furrow formation. Accordingly it appears that the Na^+-K^+ pump does not participate in the hyperpolarization of the membrane upon the furrow formation in macromeres. In high Ca^{2+}-application, the times of minimum Rm and the hyperpolarization of the membrane during the cell cycle did not always coincide with the time of furrow formation. Consequently it appears that these electrical and morphological changes are controlled by two mechanisms which are independent of each other and linked to the normal cell cycle.

INTRODUCTION

The execution of events in the cell-cycle has been studied from various aspets such as changes in intracellular pH [1–4], intracellular Ca^{2+} [5–10] and maturation promoting factor (MPF) [11–16]. In the present study, electrical measurement was applied to examine such cell-cycle phenomena. Among various electrophysiological approaches, oscillations in the membrane potential of amphibian eggs associated with fertilization have been described by many investigators [17–21, review 22]. They found that the membrane potential of the egg showed a general shift toward a hyperpolarized state at cleavage in *Xenopus laevis* [20, 21], *Rana pipiens* [23], and in *Cynops pyrrhogaster* [24, 25]. However, membrane potential and membrane resistance appeared to fluctuate during the cell cycle [23] or the recording time appeared to be short compared with whole cell cycle. Even when this did not occur, these reports confirmed the values of electrical characteristics at fertilization [20, 21] or first and sencond cleavage [24, 25], and there were a number of obscure points, such as when the membrane resistance began to increase, when it began to decrease, when the membrane potential began to hyperpolarize, and when furrow formation was initiated during the observed changes in membrane resistance. Therefore, the present study was conducted to examine these electrical changes in detail and their changes with time during cell division, focusing particularly on the relationship between furrow formation and changes in membrane potential and membrane resistance. Moreover, in order to elucidate the mechanism of membrane hyperpolarization, it was examined whether the membrane during hyperpolarization ws dependent not only on K^+ ion [3, 23, 25, 26] but also on the Na^+-K^+ pump.

Accepted October 12, 1988
Received August 4, 1988

MATERIALS AND METHODS

Macroblastomere cells were obtained from the blastocoel of eggs of the newt, *Cynops pyrrhogaster* in the morula stage (stage 7, 8) [29], by careful isolation with a hair-loop and placed in modified Holtfreter's solution (80 mM NaCl, 1.0 mM KCl, 1.2 mM $CaCl_2$, 1.2 mM $MgCl_2$, 0.36 mM $NaHCO_3$, pH 7.4) on a Sylgard slab. The cell diameter of each isolated macromere was measured on a plastic dish coated with agar at the "rounding-up" stage when the macromere became spherical. For investigating the electrical characteristics of the membrane, two kinds of perfusion solution were used: 56.2 mM Ca^{2+} solution, in which all NaCl in modified Holtfreter's solution was substituted by $CaCl_2$, and g-strophanthin (Merk) solution of various concentrations (0.03, 0.05, 0,10, 1.0 mM) added to modified Holtreter's solution, for inhibition of the Na^+-K^+ pump.

Electrical measurements were carried out using a current-clamp system (Fig. 1). The system was made by modifing the valtage-clamp system as described by Brown *et al.* [30]. For electrical recording, two glass microelectrodes filled with 3 M KCl were inserted into one macromere cell. One thick-walled electrode (resistance: 10 MΩ) was connected to a head amplifier (V) and the other thin-walled electrode (resistance: 2–3 MΩ) was connected to the output of a current-feedback amplifier (Vi) for current injection. The reference electrode was an Ag-AgCl wire immersed in 3M KCl solution, connected to an agar bridge immersed in experimental medium. The other end of the Ag-AgCl wire was connected to a current-voltage converter for current monitoring and current feedback to the feedback amplifier (Vi). The outputs of the preamplifier (Vm) and current monitor (Im) were connected to a pen-recorder (NIHON KODEN RJG 4004).

For insertion of the two microelectrodes into the macroblastomere cell, one voltage-recording microelectrode was oscillated by a brief over-compensation of the electrode capacitance. This procedure was important for obtaining a more negative membrane potential, which appeared to be a real negative potential without any leakage.

In the present examination, depolarizing pulses

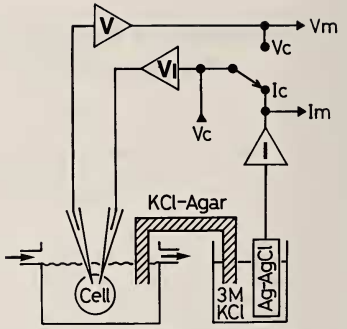

Fig. 1. Schematic representation of the circuits used for electrical measurements in current-clamp and voltage-clamp systems. In this experiment, all electrical recordings were performed under current-clamp conditions. The converted output (Ic) through the virtual ground (I) of the current-voltage converter was connected to an amplifier for current feedback (Vi) with a voltage command (Vc) pulse. V, voltage-follower for voltage recordings (Teledyne Philbrick 1332 operational amplifier). Im, current monitor. Vc, under voltage-clamp conditions, the output of the voltage-follower was connected to the voltage-feedback amplifier (Vi). The other operational amplifier was an LF356, which was used on a glass-epoxy plate with 5-mm-wide print pattern.

(duration of current-pulses, 500 msec; pulse interval, 9 sec) were used for current injection because intense rectification was observed in hyperpolarizing pulses. The membrane resistances referred to in this series mean input membrane resistances measured by the depolaizing currents.

RESULTS

Timing of the cell cycle in relation to cell diameter

In order to identify the cell-cycle stage, the timing of one cell cycle in relation to various cell sizes was first measured. The cell diameters of the isolated macroblastomeres were examined on a plastic dish coated with agar at the "round-up" stage. The sizes of the macroblastomeres obtained from the blastocoel of morula-stage eggs usually ranged from 250 μm to 500 μm, as indicated in

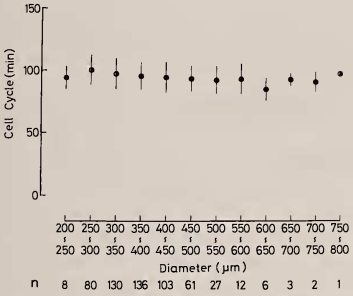

FIG. 2. The relationship between cell diameter (μm; with standard deviations) and the timig of the cell cycle (min). n; numpers of samples.

Figure 2. Cells larger than 500 μm were occasionally obtained at the early morula stage.

For identification of the cell-cycle stage, the first cleavage-furrow served as a convenient reference. Accordingly, the times of the cell cycle wer calculated from the formation of the initial cleavage-furrow to that of the next cleavage-furrow. When the timing of the cell cycle was compared between 5 ranges of cell size from 250–300 μm to 450–500 μm, the marked difference of the time was not found ($P<0.05$). Consequently, the timing of the cell cycle in used macromeres were about 96 min ($n=568$).

Timing of the cell cycle in relation to room temperature

Having established that one cell cycle took about 96 min in cells of various sizes, the dependence of cell-cycle timing on room temperature was then examined in order to identify the cell-cycle stages of cells used.

As shown in Figure 3, room temperature within a range of 22°C–28°C was classified into 4 ranges for convenience. The respective values of Q_{10} obtained were 1.16 between 22–24°C (101 min) and 24–25°C (97 min), and 1.37 between 22–24°C and 26–28°C (89 min). Consequently, at these room temperatures, the mean time of the cell cycle tended to decrease ($P<0.5$). If the time from first furow formation to second furrow formation was constant in relation to the room temperature and

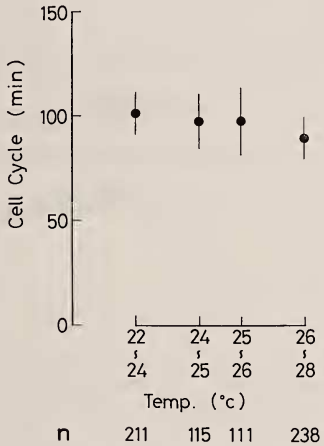

FIG. 3. The relationship between room temperature and the timing of the cell cycle. n; number of samples.

the cell sizes, an absolute time was able to designate the cell stage in the present study. However the mean time of the cell cycle was changed with the room temperature. Therefore, in the present paper, the time from first furrow formation to second furrow formation has been divided into a hundred stages, designated St.0 to St.100. The stage designations are as follows: st.50 is the start of furrow formation, and the "round-up" stage, for example, covers range from st.30 to st. 40 and the "relaxed" stage a range from st.40 to st. 45. These designations of cell stages are different from those used in previous reports [cf. 31].

Electrical measurement of the cell-division cycle

Recordings of changes in membrane potential and membrane resistance are shown in Figure 4. The time-markers in the uppermost trace (Time) correspond to the cell stages from St.0 to St.100 in these two records (Figs. 4A and B). The second traces (Im) show the intensities of the respective injected currents (A, 20 nA; B, 15 nA). The third traces (Vm) show the membrane potentials and

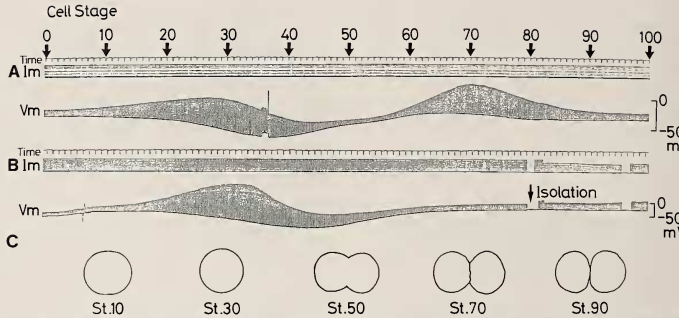

Fig. 4. Two typical recordings obtained during the cell cycle (A, B). The illustrations in C are morphological outlines of blastomere cells at each stage. Im in A indicates the intensity of the injected current (20 nA constant). Im in B is 15 nA. After the stimulation had been interrupted briefly near the arrow in B, the membrane resistance was alightly increased as a result of electrical uncoupling. The temperature was 26°C and the macromere sizes before cleavage were 500 μm (A) and 625 μm (B). The arrow in B indicates the seperation of a daughter-cell by a hair-loop. The calibration of potential is indicates on the right.

membrane resistances. Figure 4C shows schematic drawings of the macroblastomere at St.10, St.30, St.50, St.70 and St.80, respectively.

As seen in Figure 4A, the membrane resistance began to increase at about St.5, and reached an initial peak resistance (2.2 MΩ) at aobut St.30. In parallel with this increase in membrane resistance, the membrane began to hyperpolarize at about St.10 and attained a maximum hyperpolarized potential (−75 mV) at St.35. Thus, the maximum hyperpolarization potential always appeared after the first maximum membrane resistance, the time lag being about 10 min in Figure 4A. After St.30, the membrane resistance began to decrease and reached a minimum value (0.29 MΩ) at St.53, subsequently increasing again and reaching a second peak (2.1 MΩ). After the maximum hyperpolarization, the membrane potential began to depolarize and reached a plateau of Em (−36 mV) at about St.63. In the process of this depolarization, furrow formation occurred at St.50.

As seen in Figure 4B, the stage of maximum hyperpolarization potential (−84 mV) was St.44. Despite this similarity in the features of the change in membrane potential in Figure 4A and B, there was only one stage of maximum resistance (Fig. 4B). The membrane resistance began to show an increase at St.10 (0.54 MΩ) and reached maximum Rm (4.6 MΩ) at St.33, subsequently decreasing and reaching 0.89 MΩ at St.65.

The marked difference between Figures 4A and 4B was due to the changes in membrane resistance, that in Figure 4A having two peaks (St.20-St.40).

The changes in the mean membrane potentials and mean membrane resistnaces are shown in Figure 5. The membrane potential at St.0 was -53 ± 9 mV, and then the membrane became depolarized to -50 ± 11 mV at St.10. After St.10, hyperpolarization was seen, reaching a maximum of Em at St.40 (-85 ± 8 mV). When the membrane potentials had reached a value of about 90% of the maximum (St.40), the cleavage-furrow was usually formed at St.50 (-75 ± 11 mV). After cleavage, the membrane potential reached a plateau at St.70 (-50 ± 11 mV). It thus appeared to be characteristic that the maximum hyperpolarized potential occurred within about 10 min after furrow-formation.

In parallel with these changes, the mean membrane resistance began to increase from St.0 (2.3 ± 0.9 MΩ) and then increased gradually to its maximum value (4.3 ± 2.3 MΩ) at St.30. After St.30, the average membrane resistance decreased to a minimum value (1.4 ± 0.7 MΩ) at St.60 through furrow-formation at St.50, close to the time when

the decreasing Rm crossed the depolarization of the membrane. After St.60, the membrane resistance increased gradually, and finally reached 2.8 ± 1.4 MΩ at St.100, corresponding to the next St.0.

Thus, as shown in Figure 5, the average membrane resistances of the blastomere increased in two stages of the cell cycle and decreased to a minimum value at St.60, although the second increase at St.70–St.80 was not remarkable.

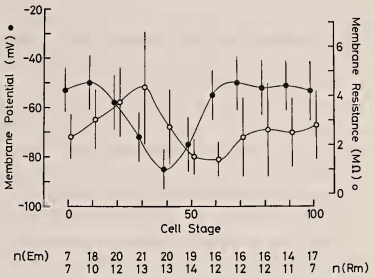

FIG. 5. Changes in the averaged membrane potential and membrane resistance, with standard devkations, during the cll cycle. n; numbers of samples.

Application of two different Ca^{2+}-rich solutions

As shown in Figure 6A-D, 10 mM $CaCl_2$ solution was perfused for a 5-min period at various stages (A, St. 0; B, St.40; C, St.60; D, St.80), resulting in membrane resistance increases of 1.7-fold, 1.6-fold, 2.9-fold and 1.5-fold, respectively, in comparison with preperfusion values of 2.9, 4.4, 1.2 and 2.5 MΩ, respectively. The values of the depolarized potential was from +12 to +14 mV in each case. Consequently, the depolarization produced by application of 10 mM Ca^{2+} solution suggested qualitatively that the membrane of the blastomere cell seemed to be most sensitive at about St.40 (Fig. 6A-D).

As shown in Figure 6E, 56.2 mM Ca^{2+} solution was applied for 5 min beginning at St.10, and the membrane potential was depolarized from −39 mV (St.10) to −24 mV after 2 min. Subsequently, the membrane potential gradually became hyperpolarized to −66 mV after 9 min, and was then

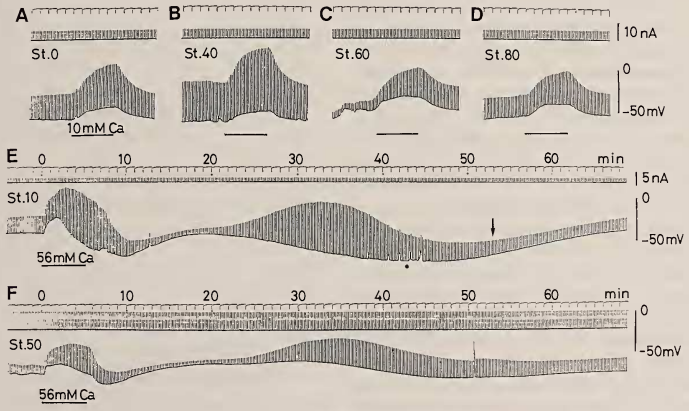

FIG. 6. The effects of Ca^{2+}-rich solutions on the membrane of blastomeres (A-D, 10 mM; E, F, 56 mM). The calibrations of current and voltage are indicated on the right. The electrical changes in E were recorded during a 113-min period from St. 10, whereas those in F were recorded during a 148-min period from st. 50. The macromere sizes were 406 μm in A-E, and 724 μm in F. The arrow head in E indicates the timing of furrow-formation. At 100 min in E, the daughter-cells sizes were 292 μm and 262 μm. After 51 min in F, the daughter-cells were separated and their sizes were 527 and 513 μm.

depolarized to −43 mV after 17 min. Meanwhile the membrane resistance increased from 4.0 MΩ (St.10) to 11.3 MΩ after 6 min, and then decreased 1.2 MΩ after 17 min.

After the application of Ca^{2+}, the features of the electrical change during 20–68 min (Fig. 6E) were similar to those before and after furrow formation (Fig. 4B), i.e., the membrane resistance increased to 11.9 MΩ after 34 min, and then decreased to 2.7 MΩ after 62 min, followed by an increase to 4.3 MΩ after 82 min, and a decrease from St.50 until 113 min. On the other hand, the membrane potential was −43 mV after 17 min, and then the membrane was hyperpolarized to −74 mV after 43 min. At 82 min after application, depolarization to −37 mV was seen, and 53 min after St.10, furrow formation occurred.

As shown in Figure 6F, 56.2 mM Ca^{2+} solution was applied for 5 min beginning at St.50, and then the membrane was depolarized from −69 mV (St.50) to −58 mV after 2 min. Subsequently the potential became gradually hyperpolarized to −80 mV after 7 min, and then depolarized to −58 mV after 18 min. Meanwhile, the membrane resistance increased from 0.51 MΩ (St.50) to 1.57 MΩ after 5 min, and then decreased to 0.25 M after 18 min. At 37 min after St.50, the membrane resistance increased to 1.61 MΩ, and then decreased to 0.79 MΩ after 65 min. On the other hand, the membrane potential was −43 mV after 22 min, and then the membrane hyperpolarized to 74 mV after 48 min. At 90 min after application, depolarization to −37 mV was seen, and 148 min after St.50, furrow-formation occurred.

Consequently, the changes occurring in membrane potential and membrane resistance during 20–68 min after the application of 56 mM Ca^{2+} solution were similar to the electrical changes shown in Figure 4B. As shown in Figure 6E, furrow formation was observed 53 min after St.10, suggesting that the timing of furrow formation was delayed for 20 min by perfusion of the Ca^{2+} solution. On the other hand, as shown in Figure 6F, furrow formation was not observed 18 min and 65 min after St.50, but did occur 142 min after St.50. In other words, the timing of furrow formation was delayed for about 50 min due to perfusion of the Ca^{2+} solution. Then, in stead of the cell stage, the times from the onset of the perfusion were used for staging the cell cycle. From the observation that cleavage furrow formation did not always occur when the membrane resistance was low and the membrane hyperpolarized, the respective mechanisms responsible for furrow formation and

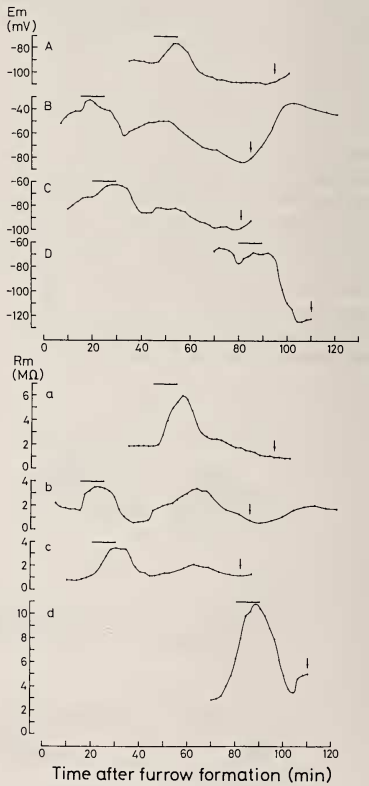

Fig. 7. The effects of Na^+-K^+ pump blocking by the 1-mM g-strophanthin for 10-min periods at various cells stages. The arrow indicate the timing of furrow-formation. The changes in the membrane potentials and membrane resistances in one recording are indicated separately in the top (A, B, C, D) and bottom (a, b, c, d) panels, respectively.

electrical changes were considered to be independent, but closely linked.

g-Strophanthin solution

The K^+ ion dependence of the membrane potential in macromeres has been previously investigated by many researchers [3, 23, 25–28]. In this study, we examined whether the Na^+-K^+ pump was present not only in whole egg [32] but also in macromeres from the blastocoel. Upon transient application of 1 mM g-strophanthin for 10 min, as indicated in Figure 7, the depolarized membrane potentials were 16 mV (A), 9 mV (B), 10 mV (C) and 9 mV (D), respectively, whereas the correponding increases in membrane resistance were 4.1 MΩ (a), 1.9 MΩ (b), 2.3 MΩ (c) and 4.5 MΩ (d). After application, both types of electrical change became irregular in comparison with the normal ones, although furrow formation was not affected, as indicated by the arrows in Figure 7. In other word, the activity of the Na^+-K^+ pump was confirmed in the membrane of macromeres.

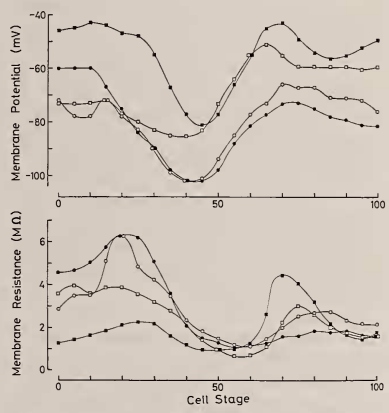

FIG. 8. The effects on the blastomere cell membrane of g-strophanthin solutions (0.03 mM, solid squares, 0.05 mM, clear squares; 0.1 mM, solid circles; 1 mM, clear circles). The membrane potential and membrane resistance are shown separately in the top and bottom panels, respectively.

In contrast with transient application of g-strophanthin, the oscillations in membrane resistance and membrane potential throughout the cell cycle were unaffected by long-term application, as shown in Figure 8. At various concentrations of the agent (0.03, 0.05, 0.1, 1 mM), the membrane was hyperpolarized up to −102 mV (0.1, 1.0 mM), −85 mV (0.05 mM) and −81 mV (0.03 mM) at about St.40 and the membrane resistance was increased in a range from 2.2 to 6.2 MΩ at about St.30. Thus the hyperpolarization potential was not influenced by inhibition of the activity of the Na^+-K^+ pump, and therefore it appeared that regulation of the membrane potential at cleavage was independent of the Na^+-K^+ pump.

DISCUSSION

In amphibian eggs, changes in the membrane potential and membrane resistance have been investigated electrophysiologically by many workers [1, 3, 17, 19–21, 23–28]. However it seems that previous investigators have generally concentrated on two main aspects, one being fertilization and additional cleavage, and the other first cleavage including aspects such as the formation of new membrane. In the present study, we restricted our investigation to oscillations in membrane parameters detected electrophysiologically during the cell cycle.

For the present purpose, we used macroblastomere cells from the blastocoel of *Cynops pyrrhogaster* egg instead of using the whole egg. This was because macromere cells seem to have uniform membrane quality without possessing certain factors such as pigments and "ion barrier" [24, 25], and also because the isolation of macromeres from the blastocoel is more convenient than obtaining pigmented macromeres from the whole egg. In spite of these advantages, this difference between unipigmented macromeres from the blastocoel and pigmented cells from the whole egg produced differences in the timing of cleavage. In pigmented cells, cleavage is seen at a time of high membrane resistance and before hyperpolarization in *Xenopus laevis* (3, 64-cell embryo; 20, 1st–5th cleavages; 21, 1st and 2nd cleavages). However in unpigmented cells from the blastocoel, cleavage

was visible as a furrow after maximum hyperpolarization. Accordingly, cleavage seems to occur later than that in pigmented macromeres. The differences in membrane resistance observed during St.60–80 (Fig. 4A and B) may be due to the presence of two kinds of macromere in the blastocoel. Thus, it may be necessary to conduct electrical examinations of vegetal blastomeres containing germ plasm situated around the vegetal pole [33, 34].

With the exception of the increase in membrane resistance during St.60–80, increases generally occurred between St.0 and St.30, as shown in Figure 5. Accordingly, it appears feasible to time furrow formation on the basis of the increase in membrane resistance, and it was revealed that preparation for the next cleavage was established at least by St.0. This consideration for furrow determination holds the similar views shown by Dettlaff units [35].

The relationships between Ca^{2+} ion and furrow formation have been reported in various aspects [5–9, 36]. Especially, it appears important whether the intracellular Ca^{2+} rises at the cleavage or not. However, in amphibian egg, there are no direct evidence for the distribution or sequential changes of the intracellular Ca^{2+} during the cleavage. If the concentration of the intracellular Ca^{2+} in amphibian egg was low at the furrow formation as well as sea urchin egg [37], the responsibility of the egg membrane to the extracellular Ca^{2+} appeared to change.

Upon application of 10 mM Ca^{2+}-rich solution, the membrane potential and membrane resistance of macromeres changed transiently. On the other hand, 56 mM Ca^{2+}-rich solution produced oscillations in membrane potential and membrane resistance during a 20-min period after application and beyond. Such electrical changes were similar to those observed in standard solution, as shown in Figure 4B. Accordingly, these oscillatory electrical changes in the membrane produced by application of Ca^{2+} solution strongly suggest that Ca^{2+} ion plays an important role in the cell cycle. Moreover, the mechanism which induces these oscillatory changes and the mechanism responsible for furrow formation appear to be independent of each other, since furrow formation did not occur even 65 min after St.50, as seen in Figure 6F. The two mechanisms seem to be closely linked in the normal cell cycle, but separable by application of 56 mM Ca^{2+} solution. Thus it suggests that membrane possess the peculiar rhythm. This phenomenon coincides with the presense of autonomous cyclic activities in non-nucleate egg fragments of amphibian eggs [38–40]. Then, it will be necessary to measure electrophysiologically for the effects of the various inhibitors as colchicine and cytochalasin B in addition to test the non-nucleate egg fragment.

It have been reported that Em of the whole egg and macromere in *Cynops pyrrhogaster* was dependent on extracelluar K^+-ion [3, 23, 25–28]. Moreover, it was reported that Na^+-K^+ pump inhibitor decreased the membrane potential [32; 41, 42: neurula embryo]. However the effect of Na^+-K^+ pump inhibitor on the hyperpolarization of the membrane at the cleavage was not examined without first cleavage [cf. 32].

The application of 1 mM g-strophanthin confirmed the transient responsiveness of the membrane to this agent in various cell stages. However, the results of g-strophanthin application throughtou the cell cycle indicated that the hyperpolarizations of the membrane potential during furrow formation and the changes in membrane resistance are not influenced. Consequently, at least during one cell cycle, the function of the Na^+-K^+ pump was found to be unnecessary for the complete passage of the cell cycle.

These facts that Em depend on external K^+-ion [3, 23, 25–28] and hyperpolization of Em at cleavage need not Na^+-K^+ pump in addition to the effect of high-Ca^{2+} ions on membrane suggest circumstantially the existence of Ca^{2+}-activated K^+ conductance [43–45].

Recordings that have been reported up to now have been obtained over short periods or with an unstable membrane resistance due to fluctuations in the microelectrode current injection. In particular, the relation between membrane resistance and membrane potential has not been described in detail. In this study, it was revealed that the membrane resistance measured using the depolarizing current had at least one single peak of high resistance at St.30 in the cell cycle, and that the

hyperpolarized membrane potential was as large as about −90 mV. For future studies on the relation between nuclear division and membrane electrical oscillation in the cell cycle, observations using a dissecting microelectrode as well as detailed histological investigation, will be necessary.

ACKNOWLEDGMENTS

We thank Dr. Katsushi Morimoto for advice during the work. This work was supported partially by Grants-in-Aid for Scientific Research from the Ministry of Education, Science and Culture, Japan (No. 59740370 and No. 61740425).

REFERENCES

1 Lee, S. C. and Steinhardt, R. A. (1981) Observations on intracellular pH during cleavage of eggs of *Xenopus laevis*. J. Cell Biol., **91**: 414–419.

2 Shen, S. S. and Steinhardt, R. A. (1978) Direct measurement of intracellular pH during metabolic derepression on of the sea urchin egg. Nature, **272**: 253–254.

3 Clack, C. and Warner, A. E. (1973) Intracellular and interecellular potentials in the early amphibian embryo. J. Physiol. (Lond.), **232**: 313–330.

4 Slack, C., Warner, A. E. and Warren, R. L. (1973) The distribution of sodium and potassium in amphibian embryos during early development. J. Physiol. (Lond.) **232**: 297–312.

5 Baker, P. F. and Warner, A. E. (1972) Intracellular calcium and cell cleavage in early embryos of *Xenopus laevis*. J. Cell Biol., **53**: 579–581.

6 Izant, J. G. (1983) The role of calcium ion during mitosis: calcium participates in the anaphase trigger. Chromosoma, **88**: 1–10.

7 Poenie, M., Alderton, J., Tsien, R. and Steinhardt, R. A. (1985) Changes of free calcium levels with stages of the cell division cycle. Nature, 147–149.

8 Poenie, M., Alderton, J., Steinhardt, R. and Tsien, R. (1986) Calcium rises abruptly and briefly throughout the cell at the onset of anaphase. Science, **233**: 886–889.

9 Keith, C. H., Maxfield, F. R., and Shelanski, M. L. (1985) Intracellular free calcium levels are reduced in mitotic PtK2 epithelial cells. Proc. Natl. Acad. Sci. U.S.A., **82**: 800–804.

10 Keith, C. H., Ratan, R. Maxfield, F. R., Bajer, A. and Shelanski, M. L. (1985) Local cytoplasmic calcium gradients in living mitotic cells. Nature, **316**: 848–850.

11 Masui, Y., and Markert, C. (1971) Cytoplasmic control of nuclear behavior during oocyte maturation of frog oocytes. J. Exp. Zool., **177**: 129–146.

12 Hara, K., Tydeman, P., and Kirschner, M. (1980) A cytoplasmic clock with the same period as the division cycle in *Xenopus* egg. Proc. Natl. Acad. Sci. U.S.A., **778**: 462–466.

13 Miake-Lye, R., and Kirschner, M. W. (1985) Induction of early mitotic events in a cell-free system. Cell, **41**: 165–175.

14 Karsenti, E., Bravo, R., and Kirschner, M. (1987) Phosphorylation changes associated with the early cell cycle in *Xenopus* eggs. Dev. Biol., **119**: 442–453.

15 Labbe, J-C., Picard, A., Karsenti, E., and Doree, M. (1988) An M-phase-specific protein kinase of *Xenopus* oocytes: partial purification and possible mechanism of its periodic activation. Dev. Biol., **127**: 157–169.

16 Gelerstein, S., Shapira, H., Dascal, N., Yekuel, R., and Oron, Y. (1988) Is a decrease in cyclic AMP a necessary and sufficient signal for maturation of amphibian oocytes?. Dev. Biol., **127**: 25–32.

17 Cross, N. L., and Elinson, R. P. (1980) A fast block to polyspermy in frogs mediated by changes in the membrane potential. Dev. Biol., **75**: 187–198.

18 Grey, R. D., Bastiani, M. J., Webb, D. J., and Schertel, E. R. (1982) An electrical block is required to prevent polyspermy in eggs fertilized by natural mating of *Xenopus laevis*. Dev. Biol., **89**: 475–484.

19 Iwao, Y. (1985) The membrane potential changes of amphibian eggs during species- and cross-fertilization. Dev. Biol., **111**: 26–34.

20 Webb, D. J. and Nuccitelli, R. (1981) Direct measurement of intracellular pH changes in *Xenopus* eggs at fertilization and cleavage. J. Cell Biol., **91**: 562–567.

21 Webb, D. J. and Nuccitelli, R. (1985) Fertilization potential and electrical properties of the *Xenopus laevis*. Develop. Biol., **107**: 395–406.

22 Hagiwara, S., and Jaffe, L. A. (1979) Electrical properties of egg cell membranes. Annu. Rev. Biophys. Bioeng., **8**: 385–416.

23 Woodward, D. J. (1968) Electrical signs of new membrane production during cleavage of *Rana pipiens* eggs. J. Gen. Physiol., **52**: 509–531.

24 Takahashi, M. and Ito, S. (1968) Electrophysiological studies on membrane formation during cleavage of the amphibian egg. Zool. Mag.(Tokyo), **77**: 307–316.

25 Ito, S. and Loewenstein, W. R. (1969) Ionic communication between early embryonic cells. Dev. Biol., **19**: 228–243.

26 DeLaat, S. W. and Bluemink, J. G. (1974) New membrane formation during cytokinesis in normal and cytochalasin-B-Treated eggs of *Xenopus laevis*. J. Cell Biol., **60**: 529–540.

27 Ito, S. and Hori, N. (1966) Electrical characteristics of *Triturus* egg cells during cleavage. J. Gen. Physiol., **49**: 1019–1027.

28 Kline, D., Robinson, K. R. and Nuccitelli, R. (1983) Ion currents and membrane domains in the cleaving *Xenopus* egg. J. Cell Biol., **97**: 1753–1761.

29 Okada, Y. K. and Ichikawa, M. (1947) External stage criteria in the development of *Cynops pyrrhogaster*. Jap. J. Exp. Morphol., **3**: 1–6. (In Japanese)

30 Brown, A. M., Tsuda, Y. and Wilson, D. L. (1983) A description of activation and conduction in calcium channels based on tail and turn-on current measurements in the snail. J. Physiol. (Lond.), **344**: 549–583.

31 Ito, S., Sato, E. and Loewenstein, W. R. (1974) Studies on the formation of a permeable cell membrane junction. I. Coupling under various conditions of membrane contact. Effect of colchicine, cytochalasin B, dinitrophenol. J. Membrane Biol., **19**: 305–338.

32 Ohara, A., Doida, Y., Murayama, K., Imaizumi, M., Marunaka, Y. and Kitasato, H. (1988) Na/K pump activity in the new membrane formed at first cleavage in *Cynops pyrrhogaster* eggs. Dev. Biol., **126**: 331–336.

33 Ikenishi, K. (1982) A possibility of an *in vitro* differentiation of primordial germ cells (PGCs) from bastomeres containing "germinal plasm" of early cleavage stage in *Xenopus laevis*. Develop., Growth and Differ., **17**: 101–110.

34 Kalt, M. R. (1973) Ultrastructural observations on the germ line of *Xenopus laevis*. Z. Zellforsch., **138**: 41–62.

35 Selman, G. G. (1982) Determination of the first two cleabage furrows in developing eggs of *Triturus alpestris* compared with other forms. Develop. Growth Differ., **24**: 1–6.

36 Timourian, H., Clothier, G., and Watchmaker, G. (1972) Cleavage furrow: Calcium as determinant of site. Exptl. Cell Res., **75**: 296–298.

37 Suprynowicz, F. A., and Mazia, D. (1985) Fluctuation of the Ca^{2+}-sequestering activity of permeabilized sea urchin embryos during the cell cycle. Proc. Natl. Acad. Sci. U.S.A., **82**: 2389–2393.

38 Sakai, M., and Kubota, H. Y. (1981) Cyclic surface changes in the non-nucleate egg fragment of *Xenopus laevis*. Develop. Growth & Differ., **23**: 41–49.

39 Hara, K., Tydeman, P., and Kirschner, M. (1980) A cytoplasmic clock with the same period as the division cycle in *Xenopus* eggs. Proc. Natl. Acad. Sci. U.S.A., **77**: 462–466.

40 Kobayakawa, Y. and Kubota, H. Y. (1981) Temporal pattern of cleavage and the onset of gastrulation in amphibian embryos developed from eggs with the reduced cytoplasm. J. Embryol. Exp. Morphol., **62**: 83–94.

41 Blackshaw, S., and Warner, A. E. (1976) Alterations in resting membrane properties during neural plate stages of development of the nervous system. J. Physiol. (Lond.), **255**: 231–247.

42 Bergman, C. and Bergman, J. (1981) Electrogenic responses induced by neutral amino acids in endoderm cells from *Xenopus* embryo. J. Physiol. (Lond.), **318**: 259–278.

43 Miyazaki, S. and Igusa, Y. (1982) Ca-mediated activation of a K current at fertilization of golden hamster eggs. Proc. Natl. Acad. Sci. U.S.A., **79**: 931–935.

44 Igusa, Y., and Miyazaki, S-I. (1986) Periodic increase of cytoplasmic free calcium in fertilized hamster eggs measured with calcium-sensitive electrodes. J. Physiol. (Lond.), **377**: 193–205.

45 Miyazaki, S-I. (1988) Inositol 1,4,5-triphosphate-induced calcium release and guanine nucleotide-binding protein-mediated periodic calcum rises in golden hamster eggs. J. Cell Biol., **106**: 345–353.